

Electron transfer and ionization in collisions between protons and the ions He^+ , Li^{2+} , Be^{3+} , B^{4+} , and C^{5+} studied with the use of a Sturmian basis

Thomas G. Winter

Department of Physics, Pennsylvania State University, Wilkes-Barre Campus, Lehman, Pennsylvania 18627

(Received 15 December 1986)

Total cross sections are reported for electron transfer and ionization in collisions between protons and the hydrogenic ions Be^{3+} , B^{4+} , and C^{5+} , and results are presented for He^+ and Li^{2+} in addition to those previously reported. Proton energies relative to the target ion are in the range 17.5–150 keV for He^+ targets, increasing with the target's nuclear charge to 150–600 keV for C^{5+} targets. Within these energy ranges the electron-transfer cross sections reach their peak values, and the ionization cross sections approach peak values from below. A coupled-Sturmian-pseudostate approach has been taken, and the largest-basis results are estimated to be converged to within 10% at energies where the electron-transfer cross sections peak. With sufficiently large bases, the cross-section curves vary smoothly and regularly with energy and the target's nuclear charge. Scaling rules for these curves are examined and compared with the simple scaling laws in the Born approximations.

I. INTRODUCTION

Electron transfer in collisions between protons and the hydrogenic ions He^+ , Li^{2+} , Be^{3+} , ... is a basic class of collision processes. With the target ion in its normal ground state, the process is nonresonant, and serves as the prototype of electron transfer from the K shell in collisions between protons and heavy ionic or neutral targets.¹ Since there is only one electron in the collisional system, the proton–hydrogenic-ion collision is amenable to a potentially accurate treatment whose underlying features can be studied unambiguously.

The electron-transfer cross section would be expected to peak at a proton speed v (relative to the target ion) which is on the order of the mean speed Z_B of the electron in the target ion of nuclear charge Z_B . (The proton and target nucleus are denoted by A and B , respectively; atomic units are used except where noted.) Even at this peak, however, the cross section would be expected to be small; it is difficult for the proton to pull the electron away from the more highly charged target nucleus—increasingly so, the greater Z_B is. Partly because of their smallness, charge-transfer and ionization cross sections have been determined both experimentally^{2–4} and theoretically^{5–10} only for He^+ targets; for higher- Z_B targets only theoretical values have been determined: coupled-pseudostate results by Winter¹⁰ and others^{11,12} for Li^{2+} targets, and strong-potential second-Born-approximation results by Macek and Alston¹³ for arbitrary *high- Z_B* targets.

The electron in transfer does not only proceed directly from the target nucleus to the proton by a simple first-order process. Rather, it can also—and, indeed, may primarily—pass through a series of intermediate states, in which it is largely unbound to either nucleus, which bridge the large energy gap between the initial and primary final state. The collisional process is thus, at least in part, second order, particularly for larger values of Z_B , at least at proton energies near where the cross section peaks, as well as at higher energies. Furthermore, al-

though at high energies a second Born approximation—particularly the strong-potential version¹³—may be expected to represent this process adequately, this is not the case at lower (peak) energies unless the target is highly charged; the latter case is tractable because $(v/Z_A)^2$ greatly exceeds unity even though $(v/Z_B)^2$ is of order unity. The most fruitful approaches to the proton–hydrogenic-ion process at intermediate energies for targets having only moderately large values of Z_B thus appear to be the coupled-pseudostate approaches,^{5–12} which represent the continuum discretely while making no assumption about the proton's speed. Indeed, with sufficiently large bases such approaches may yield an exact solution to the collisional problem.

Potentially reliable ionization cross sections are a by-product of pseudostate calculations of electron-transfer cross sections. For proton–hydrogenic-ion collisions, the ionization cross section is also small. At high energies, where ionization is much more likely than electron transfer, the ionization cross section can be determined by a first-order calculation.¹⁴ At lower intermediate energies, however, electron transfer may be more likely than ionization, particularly when Z_B is not large, and may substantially influence the ionization process. Indeed, charge transfer to the continuum may be important at lower energies, as has previously been shown to be true for proton–hydrogen-atom collisions at low keV energies.^{15–17} This process of ionization by charge transfer, as well as the process of direct ionization from the target, is accounted for automatically in double-center, coupled-pseudostate calculations with sufficiently large bases.

Previously, Winter^{9–10} employed a coupled-Sturmian-pseudostate basis to treat electron transfer and ionization in collisions between protons and the least highly charged hydrogenic ions He^+ and Li^{2+} . In the present study, sufficiently more highly charged ions— Be^{3+} , B^{4+} , and C^{5+} —will be considered so that overall trends may be established: the variation of each cross section with target nuclear charge and proton energy over about an order-of-

magnitude range of energies near where the electron-transfer cross section peaks, quantitative scaling rules with proton energy and target nuclear charge, and especially connections with the scaling laws for the appropriate first- or second-Born approximations.^{13,14}

The electron-transfer and ionization probabilities would be expected to decrease rapidly with increasing nuclear charge and, even at peak impact parameters, to be much less than unity for the more highly charged targets. This might be expected to pose problems in a coupled-state calculation: for example, insufficient numerical accuracy in integrating the coupled equations and excessive sensitivity to the size of basis. These and other potential problems will prove not to be serious for the hydrogenic targets considered, provided sufficiently large and precise calculations are carried out.

II. METHOD AND NUMERICAL TESTS

Following earlier work by Gallaher and Willets¹⁸ and then Shakeshaft^{19,15} on electron transfer in p -H collisions, Winter⁹ extended the coupled-Sturmian-pseudostate approach to electron transfer in collisions between a bare nucleus and arbitrary hydrogenic ions. The Sturmian approach has also been applied to ionization;^{19,15,10} positive pseudostate eigenvalues can be said to represent the hydrogenic continuum.

The Sturmian-pseudostate approach perhaps has the advantages of being systematic and simple. (However, it should be pointed out that any pseudostate basis is suitable if sufficiently complete for the process being studied.) The Sturmian basis is complete if sufficiently large, since it consists simply of polynomials multiplied by fixed exponentials for each angular momentum, the set of polynomials itself approaching completeness as it is enlarged. (The limiting basis is actually overly complete, since a set of functions is centered on each nucleus; problems of linear dependence have, in practice, not been encountered with the finite bases used.) The coupled equations and the matrix elements with a Sturmian basis have been described in detail by Winter in Ref. 9 and will not be repeated here.

In the remainder of this section, numerical tests will be described which provide estimates of the accuracy of the electron-transfer and ionization cross sections. As in previous work,^{9,10} most of these tests were carried out at impact parameters ρ near where the probability times impact parameter $\rho P(\rho)$ peaks. The sensitivities to various parameters are now considered as functions of the nuclear charge Z_B and the scaled proton energy $E/(25Z_B^2) = (v/Z_B)^2$ in view of the scaling rules to be presented in Sec. III B. [The proton speed in units of the Bohr velocity of the target ion is v/Z_B ; the electron-transfer cross-section curves will be seen to peak at the scaled energy $(v/Z_B)^2 \cong 0.5$.] The noted values of parameters are usually those actually employed in production runs with the larger bases.

As before,^{9,10} the coupled equations have been integrated over the variable $z = vt$ using Hamming's method.²⁰ For nuclear charges $Z_B = 3-6$, the absolute truncation error has been automatically kept between 5×10^{-6} and

5×10^{-4} ; comparison with results obtained with smaller error limits shows that the maximum estimated errors in the electron-transfer (transfer to the ground state and transfer to all states) and ionization probabilities decrease from 0.1% to less than 0.01% as the scaled proton energy $(v/Z_B)^2$ is increased from $\lesssim 0.2$ to 1.5.

The charge-exchange matrix elements, which are velocity dependent, have again been evaluated by double numerical integration over the spheroidal coordinates λ and μ . The required number of integration points for a given percent accuracy grows with both increasing Z_B and $(v/Z_B)^2$. The accuracy with the number of integration points finally used was established by comparing values of $P(\rho)$ obtained using more integration points. In general, the maximum estimated error with 12 and 24 λ point at $(v/Z_B)^2 \cong 0.1$ and 1 increases from 0.1% to 0.5% as Z_B is increased from 3 to 5. [The accuracy for ionization with $Z_B = 6$ is only 1% with 24 λ points at the tested scaled energy $(v/Z_B)^2 \cong 0.7$.] The estimated error using 16 (or 20), 24 (or 32) μ points at $(v/Z_B)^2 \cong 0.1, 1$ is generally less than 0.5% over the range $Z_B = 2-6$. [The following are exceptions for higher Z_B targets: For $Z_B = 5$ and $(v/Z_B)^2 \cong 1$, the estimated error is 2% for transfer into all states, and for $Z_B = 6$ and $(v/Z_B)^2 \gtrsim 0.5$ with 40 μ points, the estimated errors for transfer into all states and for ionization are $\leq 1\%$].

As before, the coupled equations were integrated from $z = -100 a_0$ to $+100 a_0$. By comparing results with those obtained using the larger interval from $-500 a_0$ to $+500 a_0$, the error due to restricting z to the smaller range is estimated to grow with increasing Z_B and decreasing $(v/Z_B)^2$. For $Z_B \leq 4$, the estimated error is at most 0.1%; for $Z_B = 5$, the estimated error is at most 0.2% for $(v/Z_B)^2 \geq 0.6$ while for lower scaled energies it is up to 0.8%. For $Z_B = 6$, the estimated error does not exceed 0.9%. The increasing error with increasing nuclear charge and decreasing scaled energy down to moderately low energies appears to be related to the increasing long-range polarization of the transferred electron cloud by the residual target ion.

Charge-exchange coupling was neglected for $|z| > 40 a_0$, $Z_B \leq 5$ and for $|z| \geq 30 a_0$, $Z_B = 6$. For ionization and electron transfer into all states, but not for electron transfer into the ground state, the estimated error grows with increasing Z_B . It does not exceed 0.06%, except for $Z_B = 6$, for which it is 1-2%.

After integrating the coupled equations, the summed probability is usually unity to within 5×10^{-5} . The slight departure from unity reflects the combined errors due to all the above-noted choices of parameters with the exception of the choice of the interval $(-100 a_0, +100 a_0)$; it appears consistent with the level of accuracy estimated in the electron-transfer and ionization cross sections (see below).

The total cross section Q (for electron transfer or ionization) is obtained by numerical integration (with Simpson's rule):

$$Q = 2\pi \int_0^\infty d\rho \rho P(\rho)$$

(in units of a_0^2). A sufficient number of integration points

is used—either 8–15 or 6–8 points—to ensure that the integrated cross sections are reliable to at least about 0.5% or about 1–3%, respectively.

Tabular cross sections will be reported in Sec. III. Those for which the estimated error due to each of the above-noted parameters is not more than about 0.5% are usually reported to three digits, while those for which an estimated error due to one or more of the parameters is about 1–3% are reported to only two digits.

III. RESULTS

The Sturmian cross sections for electron transfer and ionization in collisions between protons and the ions He^+ , Li^{2+} , Be^{3+} , B^{4+} , and C^{5+} are plotted in Fig. 1 and listed in Tables I–V. The results for Be^{3+} , B^{4+} , and C^{5+} are present results; for completeness, results for He^+ and Li^{2+} previously reported by Winter in Refs. 9 and 10 are also given, along with some additional results.

It is seen that the electron-transfer and ionization curves in Fig. 1 vary smoothly and simply with energy and with target nuclear charge. The absence of subsidiary structure (shoulders, minima, or additional maxima) appears to be related to the convergence of the basis, as will be described in Sec. III A. The simplicity and recurring patterns of the curves are expressible in terms of scaling rules to be presented in Sec. III B in the context of scaling laws within the Born approximations. The relation to other existing coupled-pseudostate results^{5–12} (for He^+ and Li^{2+} only) and experimental results^{2–4} (for He^+ only) will be reviewed briefly in Secs. III C and III D, respectively. Some comparison will also be made in Sec. III C with existing experimental data for *neutral C* targets.²¹

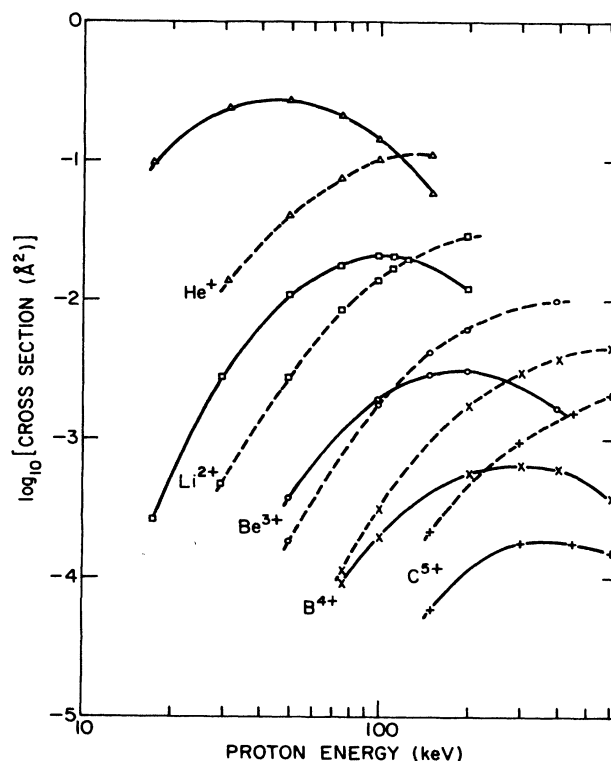


FIG. 1. Cross sections vs proton energy (relative to the target ion) for electron transfer into all states of H (solid curves) and for ionization (dashed curves) in collisions between protons and the ground-state hydrogenic ions He^+ , Δ ; Li^{2+} , \square ; Be^{3+} , \circ ; B^{4+} , \times ; and C^{5+} , $+$. The cross sections have been calculated with the larger Sturmian bases noted in Tables I–V.

TABLE I. Coupled-Sturmian cross sections (in units of Å^2) for electron transfer and ionization in collisions between protons and He^+ ions vs proton energy E [and the scaled energy $E/(25Z_B^2)$] relative to the $^4\text{He}^+$ ion. [The scaled energy is the square of the proton speed in units of the Bohr velocity of the target ion. The target nuclear charge is denoted by $Z_B (=2)$]. The collision energy with respect to the center-of-mass reference frame is $0.8E$.

E (keV)	$E/(25Z_B^2)$	Number of basis functions ^a	Electron transfer		Ionization
			$1s$	all ^b	
17.5	0.175	19 ^c	0.0917	0.0979	
17.5	0.175	35 ^d	0.0911	0.0964	
31.25	0.3125	24 ^c	0.213	0.233	0.0107
31.25	0.3125	35	0.214	0.236	0.0136
50	0.50	24	0.235	0.268	0.0379
50	0.50	35	0.230	0.272	0.0399
75	0.75	24	0.172	0.207	0.0743
100	1.00	35	0.108	0.138	0.102
150	1.50	24	0.0452	0.0611	0.108
150	1.50	35	0.0443	0.0583	0.108

^aThe 35-state cross sections at 31.25 and 100 keV and the 24-state ionization cross section at 31.25 keV are present results; the other results were reported previously by Winter in Refs. 9 and 10.

^bCross sections marked "all" are for electron transfer into all *available* bound states.

^cThe 19 functions $1sA$, $2sA$, $3sA$, $2p_{0,1}A$, $1sB$, \dots , $5sB$, $2p_{0,1}B$, \dots , $4p_{0,1}B$, $3d_{0,1,2}B$, where A and B refer to the proton and He nucleus, respectively, and the 24 functions $1s\alpha$, \dots , $6s\alpha$, $2p_{0,1}\alpha$, $\alpha = A, B, 3p_{0,1}B$, \dots , $6p_{0,1}B$.

^dThe previously defined 24 functions $+7s\alpha$, $\alpha = A, B, 3p_{0,1}A, 7p_{0,1}B, 8p_{0,1}B, 3d_{0,1,2}B$.

TABLE II. Coupled-Sturmian cross sections (in units of \AA^2) for electron transfer and ionization in collisions between protons and Li^{2+} ions vs proton energy E [and the scaled energy $E/(25Z_B^2)$] relative to the ${}^7\text{Li}^{2+}$ ion. [The scaled energy is the square of the proton speed in units of the Bohr velocity of the target ion. The target nuclear charge is denoted by $Z_B(=3)$.] The collision energy with respect to the center-of-mass reference frame is $0.875E$.

E (keV)	$E/(25Z_B^2)$	Number of basis functions ^a	Electron transfer		Ionization
			$1s$	all ^b	
17.5	0.078	26 ^c	0.000 24	0.000 27	
17.5	0.078	38 ^d	0.000 230	0.000 269	
30	0.133	36 ^d	0.002 75	0.003 21	0.000 66
30	0.133	45 ^d	0.002 61	0.002 82	0.000 48
50	0.222	26	0.0096	0.011	0.0028
50	0.222	36	0.008 80	0.0106	0.003 38
50	0.222	45	0.009 05	0.0108	0.0027
75	0.333	36	0.0155	0.0182	0.0075
75	0.333	45	0.0148	0.0177	0.0085
100	0.444	26	0.019	0.023	0.015
100	0.444	36	0.0175	0.0207	0.0139
112.5	0.500	36	0.0170	0.0203	0.0170
125	0.556	36	0.0161	0.0194	0.0195
200	0.889	23 ^c	0.012	0.014	0.028
200	0.889	36	0.009 52	0.0118	0.0285

^aThe cross sections at 30, 75, 112.5, and 125 keV, as well as the 45-state cross sections at 50 keV, are present results; the other results were reported previously by Winter in Ref. 10.

^bCross sections marked "all" are for electron transfer into all *available* bound states.

^cThe 26 functions = 19 functions (as in Table I, but for Li^{2+}) + $4sA, 5p_{0,1}B, 6p_{0,1}B, 4d_{0,1,2}B - 5sB$, where nucleus B is the Li nucleus; in the 23-function basis, the functions $4d_{0,1,2}B$ are removed.

^dThe 38 functions $1s\alpha, \dots, 7s\alpha, 2p_{0,1}\alpha, \dots, 5p_{0,1}\alpha, 3d_{0,1}\alpha, 4d_{0,1}\alpha, \alpha = A, B, + 8sB - 8s\bar{B}$; the 36 functions $1s\alpha, \dots, 6s\alpha, 2p_{0,1}\alpha, \dots, 5p_{0,1}\alpha, 3d_{0,1}\alpha, \alpha = A, B, 7sA - 6s\bar{B} + 6p_{0,1}B, 7p_{0,1}B$ at 30 and 50 keV; and the 45 functions = 36 functions + $8sA, 4d_{0,1}A, 6s\bar{B}, 7sB, 8sB, 8p_{0,1}B, 4d_{0,1}B - 8s\bar{B}$. At the higher energies for the 36-state basis, the functions $6p_{0,1}A$ are added, and $3d_{0,1}A$, removed. The line over $6sB$ or $8sB$ indicates an approximate hydrogenic state formed by diagonalizing the Li^{2+} Hamiltonian in the Sturmian basis.

TABLE III. Coupled-Sturmian cross sections (in units of \AA^2) for electron transfer and ionization in collisions between protons and Be^{3+} ions vs proton energy E [and the scaled energy $E/(25Z_B^2)$] relative to the ${}^9\text{Be}^{3+}$ ion. The collision energy with respect to the center-of-mass reference frame is $0.9E$.

E (keV)	$E/(25Z_B^2)$	Number of basis functions	Electron transfer		Ionization
			$1s$	all ^a	
50	0.125	27 ^c	4.11[−4] ^b	4.51[−4]	2.41[−4]
50	0.125	38 ^d	3.01[−4]	3.68[−4]	2.21[−4]
50	0.125	45 ^d	3.08[−4]	3.68[−4]	1.83[−4]
100	0.25	27	1.29[−3]	2.38[−3]	2.23[−3]
100	0.25	36 ^d	1.52[−3]	1.85[−3]	1.79[−3]
100	0.25	45	1.43[−3]	1.93[−3]	1.81[−3]
150	0.375	27	2.29[−3]	2.92[−3]	5.87[−3]
150	0.375	36	2.46[−3]	2.81[−3]	4.16[−3]
150	0.375	45	2.39[−3]	2.86[−3]	4.18[−3]
200	0.50	27	2.84[−3]	3.59[−3]	7.45[−3]
200	0.50	36	2.42[−3]	2.87[−3]	6.57[−3]
200	0.50	45	2.64[−3]	2.99[−3]	6.14[−3]
400	1.00	27	1.92[−3]	2.25[−3]	8.7[−3]
400	1.00	36	1.21[−3]	1.48[−3]	10.6[−3]
400	1.00	45	1.08[−3]	1.32[−3]	9.8[−3]

^aCross sections marked "all" are for electron transfer into all *available* bound states.

^bThe number in square brackets denotes the power of ten by which the preceding number is to be multiplied.

^cThe 27 functions = 26 function (as in Table II, but where B denotes the Be nucleus) + $5sB$.

^dThe 38, 36, and 45 functions as in Table II (first set of 36 functions), but for Be.

TABLE IV. Coupled-Sturmian cross sections (in units of \AA^2) for electron transfer in collisions between protons and boron (B^{4+}) ions vs proton energy [and the scaled energy $E/(25Z_B^2)$] relative to the $^{11}\text{B}^{4+}$ ion. The collision energy with respect to the center-of-mass reference frame is $0.917E$.

E (keV)	$E/(25Z_B^2)$	Number of basis functions	Electron transfer		Ionization
			$1s$	all ^a	
75	0.12	36 ^c	5.9[−5] ^b	1.2[−4]	1.9[−4]
75	0.12	45 ^c	5.2[−5]	8.3[−5]	1.0[−4]
75	0.12	55 ^d	7.1[−5]	8.8[−5]	1.1[−4]
100	0.16	36	0.77[−4]	1.9[−4]	3.8[−4]
100	0.16	45	1.4[−4]	2.0[−4]	2.6[−4]
100	0.16	55	1.4[−4]	2.0[−4]	3.1[−4]
200	0.32	36	5.0[−4]	5.7[−4]	1.4[−3]
200	0.32	45	4.3[−4]	5.4[−4]	1.5[−3]
200	0.32	55	4.6[−4]	5.5[−4]	1.7[−3]
300	0.48	36	5.6[−4]	6.6[−4]	3.0[−3]
300	0.48	45	6.1[−4]	6.9[−4]	2.7[−3]
300	0.48	55	5.2[−4]	6.3[−4]	3.0[−3]
300	0.48	60 ^e	5.4[−4]	6.3[−4]	3.0[−3]
400	0.64	36	4.4[−4]	5.3[−4]	4.0[−3]
400	0.64	45	5.0[−4]	6.0[−4]	3.6[−3]
400	0.64	55	5.0[−4]	5.9[−4]	3.7[−3]
600	0.96	36	3.0[−4]	3.7[−4]	4.3[−3]
600	0.96	45	2.5[−4]	3.0[−4]	4.3[−3]
600	0.96	55	2.9[−4]	3.6[−4]	4.4[−3]
937.50	1.50	55			4.1[−3]

^aCross sections marked “all” are for electron transfer into all *available* bound states.

^bThe number of square brackets denotes the power of ten by which the preceding number is to be multiplied.

^cThe 36 and 45 functions as in Table III, but for boron.

^dThe 55 functions = 45 functions + $9s_A, 6p_{0,1}A, 5d_{0,1}A, 8sB, 9sB, 9p_{0,1}B, 5d_{0,1}B - 9sB$.

^eThe 60 functions = 55 functions + $10s_A, 7p_{0,1}A, 10p_{0,1}B$.

A. Basis convergence studies

To explore the sensitivity of the electron-transfer and ionization cross sections to the size of basis, the number of basis functions has been progressively increased in blocks of about five or ten functions, starting with the

two-center bases of 19–27 functions defined in Tables I–III. These additional blocks of functions include s and p and sometimes d functions on one or both centers. From the cross sections listed in Tables I–V, the following conclusions may be drawn.

For a given *percent* accuracy in the electron-transfer

TABLE V. Coupled-Sturmian cross sections (in units of \AA^2) for electron transfer and ionization in collisions between protons and C^{5+} ions vs proton energy E [and the scaled energy $E/(25Z_B^2)$] relative to the $^{12}\text{C}^{5+}$ ion. The collision energy with respect to the center-of-mass reference frame is $0.923E$.

E (keV)	$E/(25Z_B^2)$	Number of basis functions ^a	Electron transfer		Ionization
			$1s$	all ^b	
150	0.167	45	4.4[−5] ^c	6.8[−5]	1.6[−4]
150	0.167	55	3.7[−5]	6.2[−5]	2.0[−4]
150	0.167	60	4.2[−5]	5.9[−5]	2.1[−4]
300	0.333	45	1.2[−4]	1.6[−4]	8.7[−4]
300	0.333	55	1.4[−4]	1.7[−4]	9.3[−4]
300	0.333	60	1.4[−4]	1.8[−4]	9.3[−4]
450	0.50	45	2.0[−4]	2.2[−4]	1.5[−3]
450	0.50	55	1.3[−4]	1.7[−4]	1.6[−3]
450	0.50	60	1.5[−4]	1.7[−4]	1.5[−3]
600	0.667	45	1.5[−4]	1.9[−4]	1.9[−3]
600	0.667	55	1.5[−4]	1.8[−4]	2.0[−3]
600	0.667	60	1.2[−4]	1.5[−4]	2.0[−3]

^aThe bases are as in Table IV, but for the target nuclear charge $Z_B = 6$.

^bCross sections marked “all” are for electron transfer into all *available* bound states.

^cThe number in square brackets denotes the power of ten by which the preceding number is to be multiplied.

and ionization cross sections, the basis must generally be larger, the larger the target nuclear charge Z_B ; the built-in scaling of Sturmian-pseudostate eigenvalues with Z_B^2 (or Z_A^2) does not in itself ensure a sufficient distribution of eigenvalues with a constant-size basis. This may be due simply to the falloff of the transition probabilities with increasing Z_B ; a small redistribution of the probability flux, in absolute terms, can significantly affect the transition probabilities, in percent terms.

Secondly, for each of the larger bases used, the last block of added states affects the cross sections ($1s$ electron transfer, total transfer, and ionization) by at most 10% near the peak in each electron-transfer cross section. At energies below the peak, the effect²² on each electron-transfer cross section is still at most about 10% down to a scaled proton energy $E/(25Z_B^2) = (v/Z_B^2) \cong 0.16-0.19$, while for ionization the effect increases to up to 23% in some cases. Above the peak, up to a scaled energy of approximately unity, the effect on the ionization cross sections actually decreases slightly (being at most 7% at this energy), while the effect on the electron-transfer cross sections grows to up to 20%.

Thirdly, in almost all cases the effect of adding successive blocks of states decreases with each successive block. (The only minor exceptions are a few changes of alternating sign, which are less serious than would be those of the same sign.) One could reasonably expect that in most cases additional untested blocks of states would affect the cross sections by less than the amounts noted in the previous paragraph.

In summary, there is an intermediate scaled-energy range where the electron-transfer and ionization cross sections are relatively insensitive to the size of basis, provided the basis is sufficiently large. Over the approximate scaled-energy range 0.18–1, the electron-transfer and ionization cross sections are probably converged to 10–20%, with the greater (10%) accuracy in the electron-transfer and ionization cross sections generally in the lower and higher parts of the energy range, respectively.²³ At lower scaled energies $E/(25Z_B^2) \cong 0.1$, all the cross sections may only be accurate to 20–30%.

It is interesting to note how smooth all the curves are in Fig. 1. This is by no means automatic: Smaller-basis results (given in the tables but not shown in the figures) in some cases exhibit more structure, presumably spurious. For example, the 36–38-state, $p\text{-Li}^{2+}$ ionization cross section displays a shoulder at $E/(25Z_B^2) \cong 0.2$, and the 55-state, $p\text{-C}^{5+}$ electron-transfer cross section displays a slight dip at $E/(25Z_B^2) \cong 0.5$ where there would otherwise be a simple maximum. [A dip was previously observed by Shakeshaft¹⁵ in the maximum of the $n=2$ cross section for direct excitation in $p\text{-H}$ collisions calculated with a scaled-hydrogenic (scaled-Sturmian-pseudostate) basis.] It appears that the sufficiently converged curves display very simple structureless forms.

B. Scaling rules

The electron-transfer and ionization cross sections for proton–hydrogenic-ion collisions (shown in Fig. 1) have simple, recurring forms: Each of the electron-transfer

curves has a single maximum, which becomes progressively lower, and occurs at a higher proton energy, the higher the target nuclear charge Z_B . The same is true of the ionization curves (although the peak is evident only for the $p\text{-He}^+$ case over the energy range shown in Fig. 1). The decline with increasing Z_B is of course related to the increasing compactness of the $1s_B$ orbital and the stronger binding of the $1s_B$ electron. The decline of the cross sections with increasing Z_B is more rapid for electron transfer than for ionization, so that whereas electron transfer substantially dominates ionization for He^+ targets over most of the energy range shown, for C^{5+} targets the reverse is true. The shape of the electron-transfer curve is almost independent of Z_B ; this is also true of the ionization curve, and suggests an unchanging mechanism for either process as Z_B is increased. This is somewhat surprising in view of the changing relative importance of electron transfer and ionization noted above and in view of the fact that electron-transfer probabilities are not very small compared to unity for all the targets. (For He^+ targets peak values are as much as 10%.) The composite intermediate state prior to breakup of the electron cloud is apparently qualitatively unaffected by increasing the nuclear charge Z_B (but see also the impact-parameter dependence to be describe later in this section).

What, if any, are the simple scaling rules with Z_B for a variational calculation¹⁵ such as the present one? At sufficiently high energies, the ionization and electron-transfer cross sections are known to be describable, respectively, by the first-Born approximation¹⁴ and by a second-Born approximation.¹³ The energy dependence of the first-Born-approximation ionization cross section (for *direct* ionization) is entirely contained in the scaled energy $E/(25Z_B^2) = (v/Z_B)^2$, whereas the energy dependence of the second-Born-approximation cross sections is contained in these terms as well as the terms $(v/Z_A)^2$. Thus the scaling with $(v/Z_B)^2$ is exact for first-Born-approximation ionization but exact only to order $(Z_A/v)^2$ [or $(Z_A/Z_B)^2$] for second-Born-approximation transfer. This nontrivial scaling is also true of the *first*-Born-approximation (e.g., Brinkman-Kramers²⁴) electron-transfer cross section, and the scaling may be expected to be even more complicated for a variational calculation such as the present coupled-state calculation with a Sturmian-pseudostate basis. Finally, the first-Born-approximation cross section for ionization contains a multiplicative factor $1/Z_B^4$, while the second- (and first-) Born-approximation cross section for electron transfer contains the smaller factor $1/Z_B^7$.

In view of these scaling considerations within the Born approximations, the Sturmian cross sections for electron transfer and ionization have been replotted in Figs. 2–4 versus the *scaled* energy $E/(25Z_B^2) = (v/Z_B)^2$. The electron-transfer cross sections in Figs. 2 and 3 (respectively, for transfer into the ground state, not previously shown, and transfer into all states) have been multiplied by the factor Z_B^7 , and the ionization cross sections in Fig. 4 have been multiplied by the factor Z_B^4 . Also shown are the first-Born-approximation ionization cross sections with exact $(v/Z_B)^2$ scaling of the energy (in Fig. 4) and the second-Born-approximation electron-transfer cross

sections (strong-potential version¹³) with approximate $(v/Z_B)^2$ scaling (in Figs. 2 and 3).

Consider first the scaled cross sections for electron transfer into the *ground* state of hydrogen, shown in Fig. 2. The Sturmian scaled cross sections are seen to be very close to one another; they are coincident to within about 10% at the peak, except for He^+ targets. (Recall the estimated 10% uncertainty in these cross sections at this scaled energy.) The greater spread at higher and lower scaled energies may in part reflect uncertainties in basis convergence, but it is probably significant that the order of the scaled cross sections with respect to Z_B is generally preserved: The *scaled* Sturmian cross sections for the most part *increase* with increasing values of Z_B . (Indeed, for the range of Z_B shown, the scaling of the cross sections is closer to $1/Z_B^{6.5}$ than to $1/Z_B^6$.) The curves approach the strong-potential–second-Born-approximation curve *from below*, but even for $Z_B=5$ and 6, the Sturmian curves are 30–40% lower at the peak and at higher scaled energies. [At lower scaled energies $(v/Z_B)^2 \cong 0.1$, the Sturmian and strong-potential–Born curves differ by about a factor of 2.] The strong-potential–Born-approximation curve peaks at $(v/Z_B)^2 \cong 0.47$ ($v/Z_B \cong 0.69$). This agrees with the location of the peak of the Sturmian curves for various Z_B : $(v/Z_B)^2 = 0.46 \pm 0.04$ ($v/Z_B = 0.67 \pm 0.03$). (The spread in the location probably reflects primarily the extent of basis convergence in the Sturmian calculations.) There does not appear to be

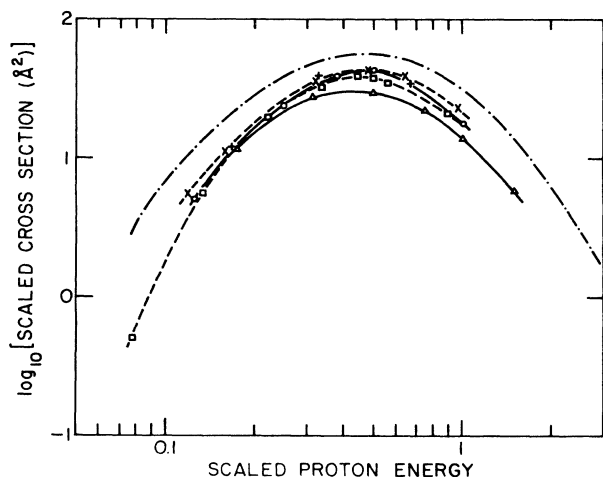


FIG. 2. Scaled cross sections $Z_B^2 Q$ vs scaled proton energy $E/(25Z_B^2) = (v/Z_B)^2$ for electron transfer into the ground state of H in collisions between protons and the ground-state hydrogenic ions He^+ , Δ ; Li^{2+} , \square ; Be^{3+} , \circ ; B^{4+} , \times ; and C^{5+} , $+$. [A C^{5+} point at $E/(25Z_B^2) = 0.5$, nearly coincident with the Be^{3+} point there, has been omitted for clarity.] These values have been determined with the larger Sturmian bases noted in Tables I–V. The solid and dashed curves are smooth curves drawn through the points except for the C^{5+} points. Dash-dotted curve is the strong-potential–Born-approximation result (Macek and Alston, Ref. 13). The target nuclear charge is denoted by Z_B . The scaled energy is the square of the proton speed relative to the target ion in units of the Bohr velocity of the target ion.

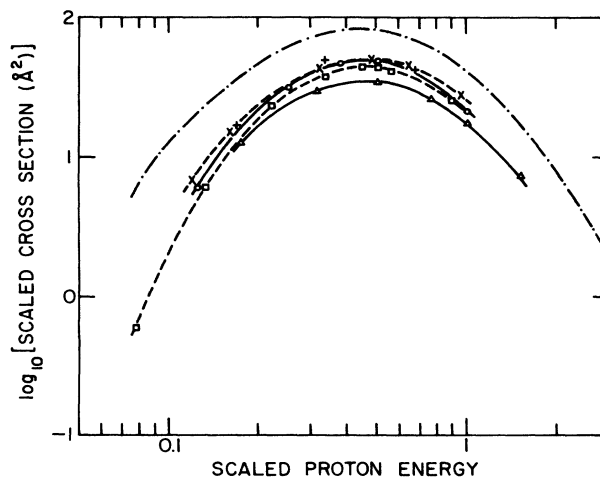


FIG. 3. Scaled cross sections $Z_B^2 Q$ vs scaled proton energy $E/(25Z_B^2) = (v/Z_B)^2$ for electron transfer into all states of H in collisions between protons and the ground-state hydrogenic ions He^+ , . . . , C^{5+} . The notation is as in Fig. 2 (a C^{5+} point at 0.5 again being omitted for clarity). The strong-potential–Born-approximation results are for transfer into *s* states only.

a simple explanation for the precise location of this peak, although an explanation would appear to involve continuum intermediate states. [The first-Born-approximation (Brinkman-Kramers) peak is located at a significantly higher scaled energy: $(v/Z_B)^2 = \frac{2}{3}$ to lowest order in $(Z_A/Z_B)^2$.]

Consider, secondly, the scaled cross sections for electron transfer into *all* states of H, shown in Fig. 3. As for ground-state transfer, the scaled curves for transfer into all states agree closely with one another, again with the exception of He^+ targets, and the trend of the curves with

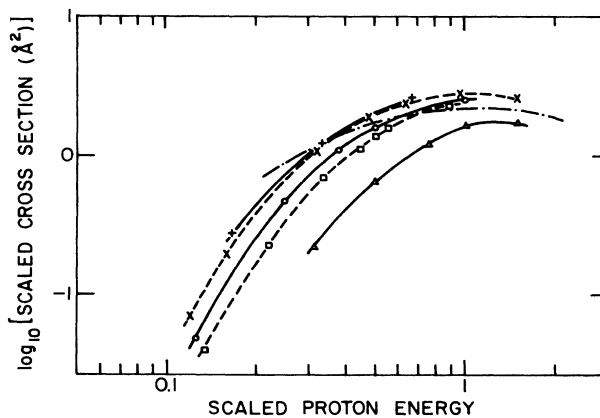


FIG. 4. Cross sections $Z_B^4 Q$ vs scaled proton energy $E/(25Z_B^2) = (v/Z_B)^2$ for ionization in collisions between protons and the ground-state hydrogenic ions He^+ , . . . , C^{5+} . The notation is as in Fig. 2 except that the dash-dotted curve is the first-Born-approximation result (Bates and Griffing, Ref. 14).

increasing Z_B is again upward. However, the difference between the higher Z_B curves and the strong-potential—second-Born-approximation curve is larger: about 70% at the curves' peak, increasing to about a factor of 3 at lower scaled energies $(v/Z_B)^2 \cong 0.1$. (Unlike the Sturmian cross sections, the strong-potential—Born-approximation cross sections are summed only over s states; the differences would be somewhat greater if p and d states were also included.) This larger difference reflects the different contribution from excited-state capture in the two treatments. In the strong-potential—Born-approximation approach, the excited-state contribution (expressed as a ratio to the $1s$ cross section) grows monotonically with decreasing energy from an n^{-3} -rule limit of 20% at high energies; the contribution is 30% at $(v/Z_B)^2 \cong 1.5$, increasing to about 75% by $(v/Z_B)^2 \cong 0.15$. The excited-state contribution within the Sturmian variational approach is more complex: For $Z_B=2$, the contribution grows monotonically with increasing energy from less than 10% for $(v/Z_B)^2 \leq 0.2$ to about 30% at $(v/Z_B)^2 \cong 1.5$. For $Z_B \geq 3$, on the other hand, the excited-state contribution has a minimum of 10–20% near the $1s$ cross section's peak, and then grows with decreasing energy to a maximum value at $(v/Z_B)^2 \cong 0.2$; the height of this maximum is roughly 20% for $Z_B=3$ and at least 30% for larger Z_B . For smaller values of $(v/Z_B)^2$, the excited-state cross section again decreases²⁵ with decreasing energy, as for $Z_B=2$. The increase of the excited-state contribution with increasing Z_B at moderately low scaled energies $(v/Z_B)^2 \cong 0.2$ seems to reflect the greater polarizing of the transferred electron cloud by a more highly charged residual target nucleus B . In the lower, nearly adiabatic energy range, capture to the ground state again appears to dominate [e.g., via a $1s\sigma$ to $2p\sigma$ transition for the p -He⁺($1s$) case]. The contribution from excited states in the strong-potential Born approximation shifts the peak in the electron-transfer cross section, summed over all (s) states, somewhat downward to $(v/Z_B)^2 \cong 0.44$ ($v/Z_B)^2 \cong 0.66$) from its value for $1s$ transfer only. For the Sturmian variational approach, the location of the peak may be largely unchanged by the inclusion of excited states: $(v/Z_B)^2 = 0.45 \pm 0.05$ ($v/Z_B = 0.67 \pm 0.04$).

Consider, finally, the scaled cross sections for ionization shown in Fig. 4. These cross sections have been multiplied by Z_B^4 rather than Z_B^7 , as suggested by the different Born-approximation factor in the case of ionization. It is seen that, as for electron transfer, the scaled cross sections generally move upward in a fairly regular way with increasing Z_B and seem to approach a limit, with the variation, however, being roughly twice as large as for electron transfer. Unlike for electron transfer, the larger Z_B curves at higher energies are above the corresponding Born-approximation curve. At the highest scaled proton energy, $(v/Z_B)^2 = 1.5$, for which ionization cross sections have been calculated, the p -B⁴⁺ cross section is 20% above the Born-approximation value, but may be merging with it as the energy is increased. (The p -He⁺ value is somewhat more than 20% below the Born-approximation value at this scaled energy.) At scaled energies below the cross sections' peak, the slopes of the

Sturmian and Born-approximation curves are quite different, the former declining more steeply with decreasing energy. The Sturmian p -B⁴⁺ ionization curve peaks at a scaled energy $(v/Z_B)^2 \cong 1.1$, which appears to be close to the peak of the Born-approximation curve; the latter's peak, however, is broader.

The Sturmian variational approach thus largely confirms the energy scaling with $(v/Z_B)^2$ for electron transfer and ionization from hydrogenic targets with nuclear charges $Z_B=2$ –6. For electron transfer and ionization, the cross sections do appear to approach the respective $1/Z_B^7$ and $1/Z_B^4$ dependences from below as Z_B is increased; these are the dependences predicted by the Born approximations. For electron transfer, the Sturmian cross sections lie below the (second-) Born-approximation curve, while for ionization for $Z_B \geq 3$ at higher scaled energies, they lie above the corresponding (first-) Born-approximation curve.

The departure of the ionization cross sections from the simple Z_B^{-4} scaling, as well as the departure from the simple first-Born-approximation curve, occurs primarily at lower energies, and most noticeably for the smaller Z_B targets. [This departure is not merely an artifact of the pseudostate calculations: experimental cross sections for the least charged ($Z_B=2$) targets (the only experimental cross sections available) will be noted in Sec. III D 1 to be in agreement.] The departure at lower energies probably reflects the importance of charge transfer to the continuum (at least for lower- Z_B targets) as well as direct ionization. Only the latter process is accounted for in the first Born approximation. A third process may also play a role at sufficiently low energies, at least for the quasisymmetric systems: the Wannier mechanism for ionization which, even more than charge transfer to the continuum, is important for p -H collisions.¹⁷ Finally, it should be mentioned that at low energies where a molecular approach should be appropriate, the charge-transferring $2p\sigma$ state would be expected to play an essential role for the quasisymmetric systems, whereas for very asymmetric systems the $1s\sigma$ state (which correlates to the ground state of the highly charged target in the separated-atoms limit) would be expected to be of primary importance. (In addition to the paper by Winter and Lin,¹⁷ see also those by SethuRaman, Thorson, and Lebeda²⁶ for p -H collisions and Anholt and Meyerhof²⁷ for heavy, asymmetric systems.)

A somewhat more detailed picture of the regularities in the electron-transfer and ionization processes may be seen in Figs. 5 and 6, respectively. In each figure, normalized probability times impact parameter $\rho P(\rho)/Q$ versus impact parameter ρ is shown at two or three representative scaled energies $(v/Z_B)^2 \cong 0.125, 0.5$, and 1 for hydrogenic targets of nuclear charges $Z_B=2, 3, 4$, and 5. It is seen that the curves are very simple and become more compact in a regular way as Z_B is increased. (Curves for $Z_B=6$ have, for clarity, been omitted; the pattern is already apparent.) At the two highest scaled energies, 0.5 and 1, there is an approximate $1/Z_B$ dependence in the location of the peak, as expected from the simple consideration of the target atom's size; the target presents a geometric area to the projectile which is proportional to $1/Z_B^2$. The

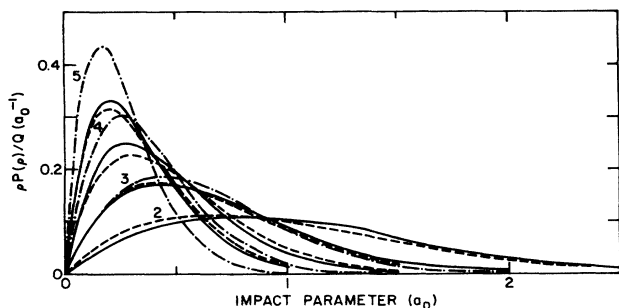


FIG. 5. Normalized probabilities times impact parameter $\rho P(\rho)/Q$ vs impact parameter ρ for electron transfer into all states in collisions between protons and the ground-state hydrogenic ions He^+ , Li^{2+} , Be^{3+} , and B^{4+} , labeled by $Z_B=2, 3, 4$, and 5 , respectively. The dash-dotted, solid, and dashed curves are for the scaled proton energies $E/(25Z_B^2)=(v/Z_B)^2 \cong 0.125, 0.5$, and 1 , respectively. (See Tables I–V for the precise energies used. The probabilities have been calculated with the larger Sturmian bases noted in these tables.) The area under each curve is $(2\pi)^{-1}$.

probability $P(\rho)$ at the peak of $\rho P(\rho)$ therefore scales approximately as $1/Z_B^5$ for electron transfer and $1/Z_B^2$ for ionization to the extent that the previously noted cross-section scalings hold at these energies. Secondly, the two higher-energy curves for a given Z_B in each figure are almost coincident and, indeed, agree fairly closely with the corresponding two curves in the other figure; this suggests that the electron-transfer and ionization processes are closely linked here.²⁸ At the lowest scaled energy $(v/Z_B)^2 \cong 0.125$, for all values of Z_B , the ionization curves are much more highly peaked than they are at the higher energies; this is only true to a lesser extent for electron transfer, and primarily only for $Z_B \geq 4$. Further, the scaling of the location of the peak of $\rho P(\rho)$ with $1/Z_B$ does not hold very well at this energy, particularly for ionization. This suggests that the electron-transfer and ioni-

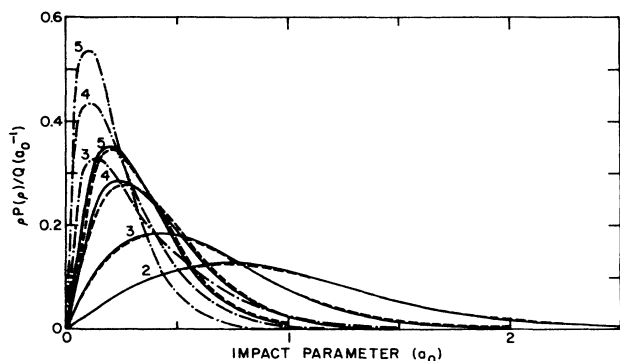


FIG. 6. Normalized probabilities times impact parameter $\rho P(\rho)/Q$ vs impact parameter ρ for ionization in collisions between protons and the hydrogenic ions with $Z_B \leq 5$ at the three scaled proton energies noted in Fig. 5, in which additional details are given.

zation processes are less strongly coupled at lower energies and especially that the breakup process is different at these energies; in particular, for lower- Z_B targets, charge transfer to the continuum may be important, as suggested in the previous paragraph. However, these observations are tentative since the Sturmian electron-transfer and ionization cross sections were only estimated to be converged to 20–30% at this lowest scaled energy.

C. Comparison with other pseudostate results

Other coupled-pseudostate results^{5–12} for hydrogenic targets, which apparently exist only for He^+ and Li^{2+} targets, have been compared in detail in Ref. 10 with the Sturmian results in that paper. Some minor changes will be noted in light of the additional Sturmian results reported here.

For electron transfer in $p\text{-He}^+$ collisions, there was noted to be excellent agreement of the Sturmian cross sections with the 16-state, augmented-atomic-orbital (AO+) results of Fritsch and Lin⁵ [to within 5% at all but the highest scaled energy, $(v/Z_B)^2=1.5$, the 15% difference there being attributed to the possible need to enlarge the comparatively small AO+ basis]. For scaled energies $(v/Z_B)^2 \geq 0.3$, about 10% agreement was noted with the 23-state, Callaway-Wooten pseudostate results of Bransden, Noble, and Chandler.⁷ (This comparison is with their results of approximation A, which employs pseudostates centered only on the proton and $n \leq 2$ bound atomic states centered on the He nucleus.) Agreement within 5–10% at the higher energies was also noted with the one-and-a-half-center results of Reading, Ford, and Becker⁸ using a large basis of 54 pseudostates with, however, only one state centered on the proton—the single 1s charge-transferring state, taken into account perturbatively. However, at the lower scaled energy $(v/Z_B)^2=0.25$, the one-and-a-half-center result is about 35% higher than the Sturmian value, which was attributed by Winter to the small number of approximate treatment of proton-centered states in the one-and-a-half-center approach.

For $p\text{-He}^+$ ionization, agreement was noted to be within 20% with the 20–23 pseudostate results of Fritsch and Lin⁶ in the overlapping energy range, and comparable agreement was noted with the one-and-a-half-center results of Reading, Ford, and Becker⁸ for scaled energies $(v/Z_B)^2 \geq 0.9$. At lower energies, the one-and-a-half-center results depart increasingly from the other two sets of pseudostate results.

For $p\text{-Li}^{2+}$ electron transfer, outstanding agreement (within 6%) was noted with the one-and-a-half-center results of Ford, Reading, and Becker.¹¹ This agreement is improved to at least 4% by the present use of a larger (45-state) Sturmian basis at the scaled energy $(v/Z_B)^2=0.222$. The two-center, 32-pseudostate results of Ermolaev and McDowell¹² agree with the Sturmian results to within 3–9% at the energy extremes and 12–25% at the intermediate scaled energies $(v/Z_B)^2=0.133\text{--}0.444$.

For $p\text{-Li}^{2+}$ ionization, the comparison with the one-and-a-half-center results¹¹ has been noted¹⁰ to be qualitatively similar to that for $p\text{-He}^+$ ionization, the two cross sections appearing to merge at higher proton energies.

Differences at lower energies, however, are substantially smaller than for $p\text{-He}^+$ ionization: a factor of 1.8 at $(v/Z_B)^2=0.222$ (with the present 45-state Sturmian basis) rather than a factor estimated to be ≥ 5 at comparable scaled energies for $p\text{-He}^+$. The preliminary 32-pseudostate results of Ermolaev and McDowell¹² are above the present Sturmian results by 22% at the highest scaled energy, $(v/Z_B)^2=0.89$, of the two calculations, the difference increasing to a factor of 2.5 at the lowest scaled energy, $(v/Z_B)^2=0.133$. This large difference at the lowest energy may be due in part to the smaller basis used in their calculation.

D. Comparison with experimental results

1. He^+ targets

There are apparently experimental cross sections for electron transfer and ionization in collisions between protons and hydrogenic ions only for the ion He^+ . These results for electron transfer and ionization²⁻⁴ were compared in Ref. 10 with the corresponding pseudostate results.⁵⁻¹⁰ For electron transfer, excellent general agreement was noted between the experimental and pseudostate results, the only significant difference probably being with the lowest-energy, one-and-a-half-center point.⁸ For ionization, it was noted that, in view of the error inherent in the experimental procedure of subtraction at lower energies (where for He^+ targets the ionization cross section is not large compared to that for electron transfer), there is probably agreement between the experimental and pseudostate results within the range of experimental error, with the exception that as the energy is decreased, the one-and-a-half-center results differ increasingly from the experimental results.

2. Multielectron targets

There do not appear to be any experimental results for other hydrogenic targets. The only other experimental results somewhat relevant to the present one-electron study are for electron transfer and ionization from the K shell of ionic Li^+ targets²⁹ and neutral C targets.²¹ In its present form, the Sturmian calculations are one electron in nature, all matrix elements involving only one-electron Coulomb potentials with constant effective nuclear charge Z_A or Z_B ; it is therefore of questionable validity to apply the Sturmian results to a multielectron target, in which the "active electron" experiences an effective nuclear force which depends on its distance from the nucleus.

Ford, Reading, and Becker¹¹ have in fact modified their one-and-a-half-center pseudostate approach to incorporate an electronic potential which accounts for variable screening by the other electrons, and they have applied this modified approach to the case of Li^+ targets. Their results for ionization agree closely with the experimental results of Sewell, Angel, Dunn, and Gilbody²⁹ for proton energies $E \geq 135$ keV, while for lower energies, where the experimental error bars are large, their results are only slightly above the experimental results. For electron transfer, on the other hand, their results are significantly

below the experimental results of Sewell *et al.* over almost the entire range of energies. They were unable to resolve this discrepancy. It is possible that the use of a screened potential in the Sturmian calculation would reduce the discrepancy with the experimental results, but this is beyond the scope of the present purely one-electron study.

The following crude analysis is within the framework of the present purely one-electron study. In order to match the maximum height of the experimental ionization cross section, the present Sturmian results imply an estimated effective charge $Z_B \cong 2.4 \pm 0.1$ for Li^+ . This same estimated effective charge would imply a Sturmian electron-transfer cross section which declines more rapidly with increasing energy than do the experimental data. The use of the effective charge $Z_B = 2.7$ predicted by Slater's rules yields a Sturmian electron-transfer curve in even greater disagreement with the experimental data. (See also the more detailed discussion following for the case of neutral C targets.)

Macek and Alston¹³ have applied their strong-potential—second-Born-approximation approach to electron transfer from the K shell of neutral C (and higher Z_B) targets by modifying the K -shell ionization potential of C to agree with the experimental value while retaining a constant effective nuclear charge (here $Z_B = 5.7$, the value predicted by Slater's rules). The electron-transfer curve agrees with the experimental data of Rødbro, Horsdal-Pedersen, Cocke, and MacDonald²¹ for proton energies $E > 400$ keV, but is above the experimental data by a factor of 2 when E is reduced to 200 keV. [It might be recalled from Fig. 3 that the scaled Sturmian results at about this energy were below the strong-potential—Born-approximation result (the purely one-electron result, without the use of the ionization potential as an additional parameter) by about the same factor.] McGuire, Kletke, and Sil³⁰ have recently calculated cross sections for electron transfer in collisions between protons and neutral C (as well as $Z_B \cong 2$ and $Z_B > 6$) targets using a version of the strong-potential second Born approximation which they state is an improvement over Macek and Alston's application of the approximation. Their results, however, are substantially farther above the experimental results than are those of Macek and Alston; McGuire *et al.* state that this poorer agreement may be fortuitous.

A rough comparison of the experimental results for C targets to the present Sturmian one-electron (fixed-screening, fixed- Z_B) results can be made as follows. The experimental data of Rødbro *et al.* should be divided by two since in neutral C either K -shell electron can be regarded as the active one. Their results for electron transfer (not shown in Fig. 1) would then lie between the Sturmian curves for $Z_B = 5$ (B^{4+}) and 6 (C^{5+}) (somewhat closer to the $Z_B = 5$ curve), while their results for ionization (not shown in Fig. 1) would lie slightly above the curve for $Z_B = 5$. What constant effective charge(s) would yield Sturmian electron-transfer and ionization curves somewhat consistent with these experimental results? For electron transfer, the *location*³¹ of the experimental peak is roughly $E = 370$ keV, corresponding to an estimated effective charge $Z_B = 5.7 \pm 0.3$ [assuming $(v/Z_B)^2$ scaling of the energy], based on the Sturmian re-

sults for $Z_B=2-6$; the *height* of the experimental peak corresponds to an estimated effective charge $Z_B \cong 5.3$ (assuming $1/Z_B^7$ scaling of the cross sections), based on Sturmian results for $Z_B=4-6$ —an only slightly smaller estimate of Z_B . The first estimate is consistent with Slater's rules. For ionization, the *location*³² of the experimental peak is roughly 720 keV, corresponding to an estimated effective charge $Z_B=5.1 \pm 0.2$ in the Sturmian calculations; the *height* of the experimental peak corresponds to an estimated effective charge $Z_B \cong 4.9$ (assuming $1/Z_B^4$ scaling of the cross sections), consistent with the first estimate for ionization. It is plausible that the average

amounts of screening experienced by electrons during electron transfer and ionization should be different, and that these amounts of screening generally exceed that predicted by Slater's rules.

ACKNOWLEDGMENTS

This work was supported by the U. S. Department of Energy, Office of Energy Research, Office of Basic Energy Sciences, Division of Chemical Sciences. All computations were performed on Pennsylvania State University's IBM 3090 computer.

- ¹A partial list of experimental and theoretical results for neutral targets of nuclear charge $Z_B \geq 6$ may be found in Refs. 13 and 30.
- ²G. C. Angel, E. C. Sewell, K. F. Dunn, and H. B. Gilbody, *J. Phys. B* **11**, L297 (1978); M. F. Watts, K. F. Dunn, and H. B. Gilbody, *ibid.* **19**, L355 (1986).
- ³B. Peart, K. Rinn, and K. Dolder, *J. Phys. B* **16**, 1461 (1983). In Fig. 6 of Ref. 10, the ionization curve of Peart *et al.* (solid curve) was inadvertently not captioned.
- ⁴K. Rinn, F. Melchert, and E. Salzborn, *J. Phys. B* **18**, 3783 (1985).
- ⁵W. Fritsch and C. D. Lin, *J. Phys. B* **15**, 1255 (1982).
- ⁶W. Fritsch and C. D. Lin, *Abstracts of Contributed Papers, Thirteenth International Conference on the Physics of Electronic and Atomic Collisions, Berlin, 1983*, edited by J. Eichler, W. Fritsch, I. V. Hertel, N. Stolterfoht, and U. Wille (North-Holland, Amsterdam, 1983), p. 502.
- ⁷B. H. Bransden, C. J. Noble, and J. Chandler, *J. Phys. B* **16**, 4191 (1983).
- ⁸J. F. Reading, A. L. Ford, and R. L. Becker, *J. Phys. B* **15**, 625 (1982).
- ⁹T. G. Winter, *Phys. Rev. A* **25**, 697 (1982).
- ¹⁰T. G. Winter, *Phys. Rev. A* **33**, 3842 (1986).
- ¹¹A. L. Ford, J. F. Reading, and R. L. Becker, *J. Phys. B* **15**, 3257 (1982).
- ¹²A. M. Ermolaev and M. R. C. McDowell (unpublished).
- ¹³J. Macek and S. Alston, *Phys. Rev. A* **26**, 250 (1982).
- ¹⁴D. R. Bates and G. W. Griffing, *Proc. Phys. Soc. London, Sect. A* **66**, 961 (1953) [in *Atomic and Molecular Processes*, edited by D. R. Bates (Academic, New York, 1962), pp. 550–556].
- ¹⁵R. Shakeshaft, *Phys. Rev. A* **18**, 1930 (1978).
- ¹⁶W. Fritsch and C. D. Lin, *Phys. Rev. A* **27**, 3361 (1983).
- ¹⁷T. G. Winter and C. D. Lin, *Phys. Rev. A* **29**, 3071 (1984).
- ¹⁸D. F. Gallaher and L. Wilets, *Phys. Rev.* **169**, 139 (1968).
- ¹⁹R. Shakeshaft, *Phys. Rev. A* **14**, 1626 (1976).
- ²⁰A. Ralston, in *Mathematical Methods for Digital Computers*, edited by A. Ralston and W. S. Wilf (Wiley, New York, 1960), p. 95.
- ²¹M. Rødbro, E. Horsdal-Pedersen, C. L. Cocke, and J. R. MacDonald, *Phys. Rev. A* **19**, 1936 (1979).
- ²²For $Z_B=2$ and 3, the estimate of error for scaled energies $E/(25Z_B^2) \cong 0.16-0.19$ has been based on the average of cross sections at two scaled energies.
- ²³Additional detailed tests for $Z_B=4$ have also been carried out at peak impact parameters—tests similar to those for $Z_B=3$ reported in Tables III and IV of Ref. 10. These tests confirm the damped oscillatory dependence of the transition probabilities for electron transfer and ionization on the number of functions of a given angular momentum and nuclear center. The oscillations, though of larger amplitude than those reported for Li^{2+} , are not inconsistent with the estimates of error reported in the text.
- ²⁴H. C. Brinkman and H. A. Kramers, *Proc. Acad. Sci. Amsterdam* **33**, 973 (1930).
- ²⁵This discounts the smaller-basis (38-state) result for $Z_B=3$ at the lowest scaled energy $(v/Z_B)^2=0.078$, and thereby alters the tentative conclusion in Ref. 10 that the n^{-3} rule (predicting a 20% contribution from excited states) is approximately valid for $Z_B=3$ over the *entire* energy range considered.
- ²⁶V. SethuRaman, W. R. Thorson, and C. F. Lebeda, *Phys. Rev. A* **8**, 1316 (1973).
- ²⁷R. Anholt and W. E. Meyerhof, *Phys. Rev. A* **16**, 190 (1977).
- ²⁸A similar remark was made previously in Ref. 10 for $Z_B=2$ and 3 only.
- ²⁹E. C. Sewell, G. C. Angel, K. F. Dunn, and H. B. Gilbody, *J. Phys. B* **13**, 2269 (1980).
- ³⁰J. H. McGuire, R. E. Kletke, and N. C. Sil, *Phys. Rev. A* **32**, 815 (1985).
- ³¹This rough estimate of the peak's location has been determined by cubic interpolation of the data points for $E=250-500$ keV.
- ³²This rough estimate of the peak's location has been determined by cubic interpolation of the data points for $E=500-1000$ keV.